

Petrology, Mineralogy and Genesis of Wadi Dana Cambrian Manganese Deposit, Central Wadi Araba Region, Jordan

El-Hasan *, T. M., Al-Malabeh**, A., Kajiwara***, Y., and Komuro***, K.

بتروولوجيه ومعدنية ونشأه خامات المنغنيز الكامبري في وادي ضانا، إقليم وادي عربه الأوسط، الأردن

طائل الحسن وآخرون

قسم الكيمياء - جامعة مؤتة

الأردن

خامات المنغنيز في الأردن تتكشف في وادي ضانا (وسط وادي عربيه)، وتكون متوضعه بشكل رئيسي داخل صخور الكامبري الأوسط. مميزات هذه الخامات البتروولوجية والمعدنية كانت هدف هذا البحث للوصول إلى معرفة نشأه وتكون التمعدن بشكل عام. والدراسة بينت وجود ظاهرة متجهية من الغرب إلى الشرق خلال طبقات الخام وذلك فيما يتعلق بشكل وتركيز ودرجة التبلور للخام، حيث لوحظ التغيير من خام قليل التركيز إلى خام عالي التركيز كلما اتجهنا إلى الشرق حتى نصل إلى جسم الخام الرئيسي في وادي ضبعه، حيث يكون الخام على شكل حزام تبلغ سماكته 2-3 م. مجموعة المعادن المكونة للخام تدل بشكل قاطع على أنه علوي النشأة. الدراسة المجهرية وكذلك المشاهدات الميدانية تدل على وجود ثلاث مراحل بنيوية للخام، المرحلة الإبتدائية وكانت سائدة في الكامبري الأسفل وتتميز بتراكمات رسوبية للخام تحت ظروف بحرية ضحلة. تبعها في الكامبري الأوسط مرحلة تكون طبقات الخام الرئيسي علوي النشأة، وهي المرحلة الأكثر شيوعاً وتطمس أو تكاد كل معالم المرحلة الأولى. وفي فترة لاحقه تأثرت الطبقات العليا من الخام بتمعدن لاحق حدثت تحت ظروف مناخية وتجوويه حادة، مما أدى إلى تكون معدن الكوروناديت وكذلك أدت إلى تركيز الحديد في هذه الطبقات العليا، بجانب هذه الأدلة دلت نتائج التحليل بواسطة جهاز (المايكروروب) على وجود سلسلة من المحاليل الصلبة بين المعادن الرئيسية للخام مما يضيف أدله أخرى على تطور الخام من خلال هذه المراحل الثلاث.

Key Words: Lower Cambrian, Manganese ore, Primary sedimentary, Supergene, Diagenesis, Epigenetic, Shallow marine.

ABSTRACT

Manganese oxides occurring at Wadi Dana (central Wadi Araba region, Jordan) are mainly hosted in the middle Cambrian dolomite limestone shale unit (DLSU). This deposit was investigated to elucidate their petrographic characteristics and genesis. The dominant mineral assemblage is typical for supergene manganese mineralization. Extensive mineralogical investigations by means of SEM and EPMA in addition to ore microscopy and field observations, allow distinguishing three genetic stages. During the first one the ore was formed primarily by sedimentary accumulations. This stage was followed by supergene enrichment, which is the dominant stage and overprints totally the primary ore features. The third stage is an epigenetic mineralization stage that affected the upper parts of mineralized horizons.

* Department of Chemistry, Mu'tah University, 61710, Al-Karak - Jordan.

** Department of Earth and Environmental Sciences, Hashemite University, Zarqa 13115, P. O. Box 150459, Jordan

*** Institute of Geoscience, Univ. of Tsukuba, Tennodai 1-1-1, Tsukuba, Ibaraki 305 Japan.

INTRODUCTION

Manganese deposits of Jordan are cropped out in two locations. First, small occurrence at Wadi Umm Ghadah - Bir Madkour, referred here as the south mineralized area, it covers the area between 30°16'-30°21'N, and 35°23'-35°29'E, (Fig. 1). The second main outcrop at Wadi Dana area, 45 km NNE of Bir Madkour area, is termed here as the north mineralized area, and has the following coordinates, 30°37'-30°41'N, and 35°28'-35°36'E, as shown in (Fig. 1). This work will concentrate on the north mineralized area. Many authors have studied these deposits [1-12]. Shaltoni (1988) [13] described the manganese mineralization of the eastern part of the area (Wadi Dabbah). Although, these deposits are known for a long time, a comprehensive and detailed study was lacking. Therefore, this work aims to investigate conclusively the whole basin of deposition (along the course of Wadi Dana). This study will be concerned on the description of the host rocks lithological facies and on the ore petrography. In addition, the study aims to investigate the mineral assemblages and textures. Consequently, attention will be placed to elucidate the ore genesis and evolution history.

GEOLOGIC SETTING

The study area is extending for about 20 km along Wadi Dana. The manganese is hosted mainly within the middle Cambrian dolomite limestone shale unit, hereafter, DLSU. Small mineralizations were found in the lower Cambrian bedded arkosic sandstone unit, henceforth, BASU. This lateral spreading was systematically sampled by covering all the basin of Wadi Dana from west to east; thus six sampling profile sites were chosen (Fig. 1). The rock formations that are exposed in the area are presented in (Table 1). The following is a general description of the study area geologic setting with more details on the manganese hosting formations. Generally the geological scene commenced with the late Precambrian - Cambrian basement, which represents the most northern appearance of the Jordanian crystalline basement. It consists of three igneous suites, the first is the Hunayk suite (porphyry granite). The second suite is the Fidan syenogranite unit (Alkali feldspar granite - Quartz monzogranite). The age of the first is about 620±14 and the age of second suite is found 538±30 Ma Brook and Ibrahim (1987) [14]. The third is Ghuwayr volcanics suite of basaltic - andesitic nature, it is found to be older than 485 Ma as reported in [12, 15, 16]. This basement has irregular terrain and it is overlain by the BASU. It starts in some areas with 3-4 m thick basal conglomer-

ate, and consists of bedded arkosic sandstone of medium - coarse grain size, brown - pinkish in color, with cross-bedding and ripple marks. Quartz pebbles of gravel size scattered randomly, and red shale intercalating the arkosic sandstone layers. The thickness is variable from one place to another; ranging 20-35 m. Few manganese mineralization is preserved in this unit as encrustation and dissemination.

The BASU is overlain directly by DLSU, which consists of fine sandstone, dolomitic sandstone, and dolomite layers intercalated with thin deep-brown and violet clay and siltstone layers. The dolomite contains less manganese mainly as secondary epigenetic veinlets or joint fillings. Meanwhile, the major manganese oxides mineralizations in this unit are associated with sandstone and claystone, as disseminations, thin bands, irregular lenses, concretions, veins, and as massive bands.

This is followed by the upper Cambrian - Ordovician sandstone (Um-Ishrin sandstone), which is overlain by the lower Cretaceous varicolored Kurnub sandstone, the upper - Cretaceous carbonates, and the Tertiary marl-silicified limestone formations. Pleistocene - Holocene basaltic floods are laying at the top. The area is highly tectonized due to the effect of Wadi Araba - Gulf of Aqaba strike-slip fault regime [2, 12, 16]. Actually the study area is located along one of the major E - W Dana shear-Fault that belongs to this tectonic regime.

METHODOLOGY

XRD survey for all samples were conducted using X-ray diffractometer at ministry of Agriculture laboratories/ Japan with CuK α radiation. The results were interpreted using JCPDS reference program. Further XRD investigations were conducted for selected ore samples after picking process under binocular microscope. This analysis was carried out using CrK α radiation machine at University of Tsukuba/ Japan. Further detailed studies were done for the main minerals using the (SEM-EDS - JOEL - JSM 5400) in addition to the (JOEL-JXA 8621) EPMA Superprobe at the Analytical Center of the University of Tsukuba. The microprobe analytical conditions were 1(10 -8 mA, 25-50 nA specimen current potential, 10 second integration time, and 20 kV acceleration potential, the SPI mineral standards were used for the calibration process. The carbon coating of the samples was prepared at the same place. The polished sections were studied under reflected and transmitted light.

RESULTS

Here there will be given a systematic petrographic

description of the different ore mineralization. Primarily, the ore was classified into two ore types, based on their Mn content. Followed by detailed mineralogical investigation including the mineral chemistry results of the main ore minerals, and describing the gangue mineral interrelationships.

TYPES OF ORE

Regarding the ore petrography, the field investigations show that there is a trending feature of the ore shape, grade, and degree of crystallinity from west to east (Table 2). The ore developed from mainly disseminated type in the west gradually towards the east, becoming lenses, thin alternating beds, concretions, until it ended at the most eastern site at Wadi Dabbah as massive 2-3 m thick band. At the same time, the ore grade is increasing in the same direction. Besides that, the degree of crystallinity shows a noticeable increase in the same trend. The mineral assemblages at the eastern high-grade ores are more clear and definite with less amorphous phase. Therefore, according to the average amount of ore grade (Vol. % of Mn) the ore can be divided into low and high-grade ores. The low-grade ores are characterizing the western sites (Wadi Khaled, Wadi Dana (the camp), Wadi Jamal, and Wadi Qusieb) at which the average grade ranges between 3.44 and 7.21 (Vol. % of Mn). The high-grade ore found at the eastern sites (Wadi Mahjoob and Wadi Dabbah) and having average ore grade between 25.6 and 26.1 (Vol. % of Mn) respectively.

Low-grade ores:

This type of ore occurs in the following shapes.

Disseminated ores: it is mainly concentrated at the western sites. Primary Mn oxides are disseminated within the sandstone and dolomitic sandstone. In hand specimen irregular disseminated bodies of Mn-cementing the sandstone are recognized (Fig. 2a). In addition to the honey bee-like texture that have been found in sandstone and dolomitic sandstone (Fig. 2b). Within this type of ore minerals phases usually has poor crystallinity.

Irregular bodies & lenses: this ore type is usually developed from the disseminated ore type. It seems that due to diagenesis the disseminated Mn oxide bodies later were connected together to form those bigger and irregular shapes. Their size ranges 0.5-2 cm (Fig. 2c). They resemble the digital concretions. Mainly composed of cryptomelane and psilomelane, with poor crystallinity. Few lenses of 20-30 cm long and 5-10 cm thick were found embedded in sandstone and clay layers. These lenses are highly fractured, and usually contain some gangue miner-

als such as kaolinite and quartz.

Thin alternating beds: the thickness ranges from 1-5 cm. Intercalated with sandstone and clay layers (Fig. 2d). This kind of ore is mainly found at Wadi Khaled, it shows high Fe content, which resembles the banded iron formation. Mineralogically, although it shows a very poor crystallinity, but there are XRD indications for cryptomelane and hollandite.

High-grade ores:

The high-grade ore existing in the following shapes.

Concretions: this type of ore is found embedded in the sandstone and red clay layers. Usually found in single form, sometimes binodular or aggregates, (Fig. 2e). Their diameter ranges from 5-10 cm. They are spherical or elliptical in shape and usually contain much quartz particles concentrated in the center that looks like a nucleus (Fig. 2f). This type of ore is mainly outcropping at Wadi Mahjoob. The mineral constituents are mainly cryptomelane, psilomelane, and pyrolusite. Some concretions show a rhythmic texture of pyrolusite and psilomelane.

Massive ore (bands): mainly found at Wadi Dabbah ore body, which are composed of massive band 2-3 m thick (Fig. 2g), with limited lateral spread. In this regard, it looks like a large lense. The mineral constituent is very complicated, and shows intimate growth of cryptomelane, hollandite, psilomelane, pyrolusite, and hematite.

Vein ore: stock-work veins are found in the upper most parts of DLSU at Wadi Mahjoob and Wadi Dabbah. They are discontinuous and intersected veins introducing the medium-coarse grained sandstone (Fig. 2h). The minerals constituents are mainly psilomelane, coronadite, hematite, and goethite. Beside coronadite, which is confined to these veins that indicate a later stage of mineralization due to lateritization or extensive weathering. In the other hand, another type of vein mineralization was found in the lower Cambrian BASU at Wadi Jamal, it consists of psilomelane and pyrolusite. In addition, it comprises oolites that consist of highly altered todorokite and birnessite. The oolitic mineralization is of microscopic sizes that have been found hosted within the stock-work veins introducing the BASU at Wadi Jamal. These oolites are mostly circular in shape with elliptical or kidney-like form, and found embedded into calcareous matrix (Fig. 3a). Since it was restricted to the BASU, thus it has significant genetic indications. Moreover, its mineralogical constituent that composed mainly from altered todorokite and birnessite. These two phases are confined to this type of ore. They are highly modified due to dia-

genesis, and replaced by psilomelane and cryptomelane. This was evident from the EPMA results, which shows an obvious solid solution between todorokite and psilomelane (Fig. 4).

Petrography and Mineral Chemistry

Manganese Minerals:

The Mn-oxides are chemically complex due to the arrangement of the MnO₆ octahedrons. Burns et al., (1997) [17] stated that the attachment of these octahedrons would form tunnel structures in between of them. The stabilization of these tunnels achieved by the filling with one or more ions like Ca⁺², Na⁺¹, K⁺, Ba⁺², Zn⁺², and Pb⁺⁴. The identity of the mineral that would have formed depends on the availability of each ion in the environment of deposition, in other words, if access of K⁺ is presented this would form cryptomelane, if Pb⁺² is available then coronadite will be formed, etc. Post et al. (1987) [18] have indicated that water may occupy these tunnels. Moreover, Post and Burnham (1986) [19] added that minor amounts of Ce and La could enter these tunnels too. Carlos et al (1993) [20] stated that the chemistry of these minerals varies over a short distance in relation to the water chemistry. Thus, partial or complete solid solution is oftenly recorded to exist between these isostructural minerals (hollandite, cryptomelane, and coronadite). Bearing this in mind, the following is a discussion regarding the mineral chemistry of the ore mineral phases.

Although the most important manganese minerals are cryptomelane, psilomelane, hollandite, and pyrolusite, but todorokite and birnessite will be described first because they have been found in the lower Cambrian (BASU) and thus represent the primary mineralization assemblage. Similarly, Ostwald (1982) [21] has described todorokite as primary mineral phase in Groote Eylandt manganese deposit. The todorokite and birnessite did not show strong X-ray diffraction lines. However, the 7Å and 10Å peaks, which are indicative for them, were frequently recognized in some charts. The qualitative SEM and quantitative EPMA results supported the X-ray charts, thus confirming their presence. They occur in the oolites, where todorokite and birnessite were totally overprinted by the diagenetically formed psilomelane (Fig. 3b). The EPMA data of todorokite show unusual enrichment of Ba, to the extent that it could be considered as Ca-rich psilomelane (Table 3). This variety of todorokite is very rare. Burns and Burns (1979) [22] reported similar Ba-todorokite from Huttenberg (Austria). Ba-todorokite might be the precursor of psilomelane as suggested by Ostwald (1988)

[23]. This might be the case in our deposit as well, where psilomelane crystals are overprinting the todorokite. Ca, Na, and K concentrations of todorokite show inverse relationships with Ba from the center toward the rims of the ooid, that indicates todorokite - psilomelane solid solution, such results were shown in (Fig.4a). The general formula of todorokite is (Ba 0.58-0.74 Ca 0.14-0.65 Na 0.052-0.16 K 0.011-0.022) Mn₈O₁₆ .xH₂O.

Cryptomelane is the main ore mineral, it is found in all ore types associated with pyrolusite and hollandite. They form the colloform and massive or blocky textured association. Very clear XRD charts of cryptomelane were found mainly in the high-grade ore samples. Cryptomelane has a variable K/Ba ratio (1-4), such variability demonstrates solid solution towards psilomelane, that is illustrated in (Fig. 4b). Moreover, it has various amounts of Na and Mg, where Na appears to substitute for K. Cryptomelane contains less water than hollandite and pyrolusite, and contains significant amounts of Cu and Zn, with traces of Ni and Co (Table 4). Petrographically, cryptomelane is oftenly replaced by psilomelane and form a solid solution that can be demonstrated in the following formula (K 0.027-0.38 Ba 0.052-0.21 Fe 0.014-0.53) Mn₈O₁₆ .xH₂O.

Psilomelane usually associates cryptomelane in the colloform or in the normal replacement texture. Moreover, it forms with pyrolusite the ring wood texture, which indicates the incrimination mode of accumulation (Fig. 3c). As mentioned previously, in BASU mineralization psilomelane is usually replacing todorokite and cryptomelane, which is evident from the wide range of K, Ba, Ca, and Na concentrations. In the upper parts psilomelane is replaced by coronadite, which marks another stage of ore formation (epigenetic). Moreover, secondary psilomelane veinlets were found invading the old psilomelane and cryptomelane (Fig. 3d). Additionally, psilomelane is associating the hematite in the secondary stock-work veins of the upper mineralized parts. It has a very high Ba/K ratio and contains high Si, Al, Ti and Fe, in addition to mild Cu content.

Hollandite similar to psilomelane mainly associates cryptomelane in forming the colloform texture, which is recorded more oftenly from the upper mineralized horizons. Hollandite has a wide variation in Fe content ranging from 3-11 wt %. The Fe₂O₃ in hollandite can reach up to 11.55 wt % as reported by Fleischer (1964) [24]. High amounts of Si, Al, Ca and K were observed. It is believed that Si and Al are substituting the Fe, while Ca

and K substitute Ba. Higher Cu concentrations were recognized up to 2.3 wt %. Also it contains traces of Co and Ni (Table 5).

Pyrolusite is restricted to the high-grade and good crystallinity ore sites. Thus, it is mainly found in the assemblages of Wadi Mahjoob and Wadi Dabbah. Pyrolusite is found as white and sometimes beige-color, and shows a blocky texture associated with cryptomelane and psilomelane. At Wadi Dabbah ore it is associated with hematite and forms the fish-scale texture (Fig. 3e). Pyrolusite contains black inclusions and cracks that form the dendritic texture, which is commonly found in supergene manganese ores. Sparse manganite remnants were recognized associating the pyrolusite blocky crystals. In the study area pyrolusite contains high amounts of Fe. It appears to contain about 10 wt% H₂O, which is similar to the Nikopol manganese deposit, Gryaznov and Danilov (1980) [25]. Additionally, significant amounts of K, Ba, and abnormal Cu concentration up to 2wt % were detected, as well as traces of Zn, Ni and Co. The blocky variety contains less than 0.1 wt% of Na₂O, that is equivalent to pyrolusite II of the Australian Groote Eylandt manganese deposit that was described as diagenetic pyrolusite by Ostwald (1988) [23]. Table 4 shows the EPMA data for selected samples from the study area, it shows a wide diversity in the trace elements contents, which can be explained by the extensive and successive diagenetic processes.

Coronadite is restricted to the upper most portion of DLSU, particularly found in the two areas Wadi Khaled and Wadi Mahjoob. In the former it is associated with secondary copper (chrysocolla) as black veinlets (Fig. 3f), while in Wadi Mahjoob it consists of the well developed and good crystallized variety, showing perfect colloform texture (Fig. 3g). The latter type resembles the coronadite of the Timna manganese deposit (Bar-Matthews 1987) [26]. Nevertheless, the coronadite of the study area is not a pure mineral such as that reported from Ekaterininsk, (formal USSR), or Imini deposit of Morocco, but rather it is a solid solution version (Table 5). It is more likely formed by the replacement of hollandite by Pb-rich solutions. Many authors [26, 27, 28] have reported such type. Moreover, Frenzel (1980) [29] had stated that in most cases coronadite resulted as a product of simultaneous weathering of Mn and Pb bearing minerals, which caused the replacement of the Mn of ore horizons by Pb. The solid solution is illustrated in the ternary plot (Fig. 4c). According to the EPMA data the general formula of coro-

nadite is (Ba 0.03-1.06 K 0.04-1.52 Pb 0.13-0.74) Mn₈O₁₆ · xH₂O.

Amorphous Mn oxide (wad) is repeatedly found. It indicates the role of diagenesis in the transformation of Mn-oxides, which affects the Mn and other cations forcing them to remobilize, thus leaving a destroyed structure hard to be identified through XRD. This process was mentioned by Sreenivas and Roy (1961) [30], they stated that (-MnO₂ minerals, i.e. psilomelane, cryptomelane, hollandite, and coronadite are stable only with strange cations such as Na, K, Ba, and Pb. If these cations were removed or leached the structure will break down.

Gangue Minerals:

Hematite is the main gangue mineral in the ore assemblage. It is a common mineral together with goethite in supergene Mn deposits. Therefore, many workers [20, 31, 32, 33, 34] had classified it as a supergene mineral. In the study area hematite was identified and detected by ore microscopy and XRD, it is found associated with cryptomelane and pyrolusite, and as secondary veinlets with psilomelane in the upper mineralized parts.

Apatite was found associating the Mn oxides at the low-grade ores of the western sites. It appears only at Wadi Khaled and Wadi Dana. It is found as carbonate-apatite, micritic, and disseminated within dolomite and siltstone. Moreover, apatite found as flaky or fibrous crystals, vary in color from pale green to yellow. SEM figures reveal a micro-lamination of Mn and Fe, where phosphorus is associated with Fe-rich lamination. Many workers had reported the close relationship of Fe and P. The secondary Mn veinlets found as veins introducing the apatite-dolomite mixed matrix.

Calcite is also associating the Mn oxides, mainly as secondary component, as vein and joint fillings. In some cases, calcite is cementing the fragmented Mn oxides, beside secondary epigenetic veins of calcite were recognized. Calcite thin microfilms are associating the hematite and pyrolusite, which would indicate another syngenetic calcite formation.

Dolomite is a host rock of the Mn minerals. Beside that, it was detected within the ore assemblage. Usually manganese mineralizations in dolomitic beds are found as secondary veins or dendritics (Fig. 3h). Secondary dolomite veinlets are found introducing the matrix, they show good crystals of perfect cleavage. Rarely, ankerite and kutnahorite were detected in few samples by XRD, without confirming them under microscope.

Clay minerals, mainly kaolinite, are often found within

the Mn-oxides assemblages, smectite and illite were detected too. Very few dark brown to pale yellow, granular bodies of glauconite-like pellets were found associating the kaolinite and quartz crystals. These pellets are more likely to be smectite rather than glauconite, because the later is common in deep marine sediments, while smectite is usually associating the shallow marine sediments Ostwald and Bolton (1992) [35]. Red clays are highly affected by the remobilized Mn-rich solutions, and they are partially replaced by manganese, that give rise to amorphous phases.

Quartz is presented in all assemblages as major gangue constituent. Medium - coarse grained, anhedral-subhedral, sometime rounded crystals, strained structure are oftenly observed, due to the high oriented pressure because of the heavy weight of the overlain rocks. Few quartz crystals were removed and filled with secondary calcite or clay minerals. Secondary Mn minerals filled highly fractured quartz crystals. Therefore, wide range of replacement by Mn oxides was recognized ranging from partial to total replacement. Other gangue minerals such as barite, K-feldspar, zircon, sphene, plagioclase are recorded under the microscope or by XRD. Amireh (1987) [36] reported the presence of brookite and dickite. Such enrichment of various minerals reflect the shallow marine environment of the depositional basin, and its approximation to the Precambrian - Cambrian complex basement.

Ore Paragenesis

The ore paragenetic sequence was deduced based on the mineral textures, in addition to mineral chemistry results, they show the ore formed in three stages. The first stage is the syngenetic sedimentary accumulation found as sparse remnants or small batch in the BASU. It is characterized by the oolitic and interstitial Mn-oxides cementing the lower Cambrian sandstones. The main minerals are todorokite and birnessite. Manganite remnants, together with quartz, dolomite, and kaolinite, may represent this. Moreover, apatite belongs to this stage, because it is usually associated with the primary ores.

Followed by the supergene enrichment stage, which developed as a result of sea level change. Consequently the physico-chemical conditions mainly the Eh and pH would change and cause the dissolution of the primary phases and the formation new phases under the new Eh-pH condition. The supergene stage is the dominant and overprinting the former stage. It shows different sort of

textures due to different mode of formation. We used the new definition of supergene that has been introduced by Nicholson (1992) [37], where he consider the process that might take place in marine environment under ample oxic conditions as a supergene enrichment process. This stage can be divided into early and late diagenetic. The main minerals of this stage are cryptomelane, psilomelane, hollandite, and pyrolusite, beside the hematite and goethite. Many workers [21, 23, 34, 37, 38] suggested this assemblage to form as a result of the secondary supergene processes of primary ores. Calcite and barite can be categorized in this genetic stage as evident from textural features.

During diagenesis large-scale replacement of country rock components, e.g. quartz, kaolinite, and dolomite, were affected the by Mn-rich solutions. Thus, the formation of kutnahorite and ankerite belongs to the early diagenesis, due to the interaction between country rock and Mn-rich solution that resulted from the remobilization and dissolution of the primary manganese ores due to the change in Eh-pH conditions. Therefore, the amorphous Mn phases would mark the beginning of the early diagenetic episode of the supergene stage.

Cryptomelane, psilomelane, pyrolusite, and hollandite show two generations. First, the early diagenetic indicated from colloform and interstitial textures. The second generation is the late diagenetic form by the modification of the former phases, and found as massive well-developed crystals. It is common to recognize poor and good crystalline phase together, which reflects the effect of diagenetic process in destroying the old and forming new phases. Pyrolusite and psilomelane dominated the late diagenetic stage, through replacing cryptomelane and hollandite, hematite was associating the assemblage of this stage. The ring wood and fish scale textures illustrated in (Figs. 3c and e) are indicative for this stage of supergene ore formation. The last stage of the ore evolution is the epigenetic stage resulted from weathering or lateritization. The effect of this stage concentrated in the upper horizons. It is hardly distinguished from the late diagenetic stage through minerals texture alone. The lateritization process caused the formation of coronadite and hollandite-coronadite solid solutions, with some association of hematite and goethite. The occurrence of specific minerals such as coronadite in certain horizons was the indicator for this stage (i.e. epigenesis). Interestingly, psilomelane and barite secondary veinlets were found introducing these phases as shown in (Fig. 3c). Hematite

as well as goethite was found associating the secondary psilomelane in the upper most horizons, which may indicate the formation by extensive weathering processes (i.e. lateritization). The presence of hematite and goethite would indicate that this stage was governed by chemical weathering, which most likely took place under humid and wet climate. Therefore, the descending meteoric water leached Cu, Pb, and Zn from rich overlying layers. This descending solution replaces the existed mineral phases and causes the formation of coronadite in the upper zone. The same solutions caused the leaching of Mn and Ba downward forming the secondary psilomelane and barite veinlets.

Obviously, the supergene minerals are the dominant over all sites and ore types. Primary sedimentary ore type was evident from the remnants of Mn mineralization preserved on the BASU at Wadi Jamal. As mentioned previously, these minerals suffered from high replacement rates by the newly formed supergene Mn oxides. The proposed paragenetic sequence represents the major constituents of both Mn-oxides and gangue minerals are illustrated in (Fig. 5).

CONCLUSION

The study lead to the following conclusions:

1. Manganese oxides embedded in the lower and middle Cambrian formations of Wadi Dana are of shallow marine type of origin.
2. There is a trending feature among the mineralized horizon throughout the study area from west to east in terms of their shapes, grades, and degrees of crystallinity. The ore gradually changed from low-grade in the western sites to high-grade in the eastern sites. The main ore body is located at the eastern part and can be described as a massive band 2-3 m thick having the highest grade up to 27 % of (Mn) as volume percents.
3. Both textures and field observations show evidences for three genetic stages of the ore evolution, primary sedimentary accumulation, secondary supergene stage that may be divided into early and late diagenetic, and lastly the epigenetic stage. The later stage took place contemporaneously with the extensive weathering of the upper parts, which cause the formation of coronadite.
4. The mineral assemblage and textures indicate the domination of secondary supergene assemblage. The main mineral constituents are the tetravalent Mn-oxides (pyrolusite, cryptomelane, psilomelane, hollandite, and coronadite).

5. The role of Eh-pH conditions as a limiting factor in all these stages is recognizable. Particularly the Eh as this deposit was formed in shallow marine environment.
6. Besides the textural features mineral chemistry provide us with additional evidences for the ore evolution stages, though the solid solution between the main mineral phases, which marks these evolution stages.

ACKNOWLEDGMENT

The authors would like to express their deep thanks to Dr. Ghazi Saffarini / University of Jordan for his continues advice and encouragement. As well the authors are deeply appreciated to the friends in geochemistry division / NRA-Jordan for their valuable help in accomplishing the fieldwork. Thanks also are due to Mr. Omar Khushman / Mu'tah University for his help and encouragement, and to Mr. Saed Shaltoni for his support and kind supply with samples and photographs. Our deep thanks to Mr. Nishida / analysis center- University of Tsukuba for his kindness and help.

REFERENCES

- [1] **Blacke, G. and Ionides, M., 1939.** Report of the agent resources of Trans-Jordan. Crown agent for colonies, London, P 371.
- [2] **G.G.M., 1966.** German Geological Mission in Jordan 1961- 1965: Final report, Unpubl. Report, Geol. Surv. of Fed. Rep.of Germany and Natural Resources Authority, Amman, Hannover, P 82.
- [3] **Basta, E.A. and Sunna, B., 1970.** Mineralogy and mode of occurrence of copper ores in wadi Araba, Jordan. Extrait du Bulletin del Institute de Egypte. 11: 197-225.
- [4] **Basta, E.A. and Sunna, B., 1973.** The manganese mineralization at Finan district, Jordan. Bulletin of Faculty of Science- Cairo Univ. 44: 111-126.
- [5] **Nimry, Y., 1967.** The manganese occurrences at Wadi Dana/ Jordan, NRA, Unpubl, report, P 62.
- [6] **Nimry, Y., 1973.** The copper and manganese prospects of Wadi Araba, NRA, Unpubl. Report.
- [7] **Burgath, K. P., Hagen, D., and Siewers, V., 1984.** Geochemistry and Geology of primary copper mineralization in Wadi Araba, Jordan., Geol. JB. 53: 3-53.
- [8] **Saffarini, G.A., and Lahawani, Y., 1990.**

- Multivariate statistical techniques in geochemical exploration applied to Wadi sediments data from an arid region: Wadi Dana, SW Jordan., *J. of African Earth Science*. 14: 417-427.
- [9] **Khoury, H. N., 1986.** On the origin of stratabound copper-manganese deposits in Wadi Araba, Jordan; *Dirasat. Amman*.13: 227-247.
- [10] **Khoury, H. N., 1989.** Industrial rocks and minerals in Jordan, (occurrences, properties, and origin), Univ. of Jordan Publ., Amman, P 240 (In Arabic).
- [11] **Lahawani, Y., and Saffarini, G., 1992.** Water soluble salts in the Mn and Cu mineralization horizons of Wadi Dana (Jordan) and their genetical bearing In: (Saffarini et al. Eds): *Geology of Jordan and adjacent area*. 3rd Jor. Geol. Conf., 395-408.
- [12] **Barjous, M.O., 1994.** The geology of the Ash Shawbak area. *Geol. Mapping Div. Bull.* 19, N.R.A. Jordan.
- [13] **Shaltoni, S., 1988.** Geochemical characteristics of the Mn mineralization at Wadi Dana area/ South Jordan., M.Sc. Thesis, Univ. of Jordan., Amman, P130.
- [14] **Brook, M., and Ibrahim, K., 1987.** Geochronological and isotope geological investigation of the Aqaba basement complex of southern Jordan. *British Geological Survey Isotope Geol. Unit Report*.
- [15] **McCourt, W., and Ibrahim, K., 1990.** The geology, geochemistry and tectonic setting of the granitic and associated rocks in the Aqaba and Araba complexes of southwest Jordan. *Geol. Mapping Div. Bull.* 10, N.R.A., Jordan.
- [16] **Rabba, I., 1994.** The geology of the Al-Qurayqira (Jabal Hamra Faddan), Map sheet No. 3051 II, Geology Directorate/NRA, Amman, Bulletin 28: P 58.
- [17] **Burns, P. G., and Burns, V. M., 1987.** Post Depositional metal enrichment processes inside manganese nodules from the north equatorial Pacific., *Earth Planet. Sci. Lett.* 39: 341 - 348.
- [18] **Post, J.E., Von Drelle, R.B., and Buseck, P.R., 1982.** Symmetry and cation displacements in hollandite: structure refinements of hollandite, cryptomelane and priderite. *Acta Crystallogr.* B38: 1056-1065.
- [19] **Post, J.E., and Burnham, C.W., 1986.** Modeling tunnel-cation displacements in hollandites using structure- energy calculations. *Am. Minerol.* 71: 1178 - 1185.
- [20] **Carlos, B. A., Chipera, S. T., Bish, D. L., and Carven, S. J., 1993.** Fracture-lining manganese oxide minerals in silicic tuff, Yucca mountains, Nevada, U.S.A., *Chem. Geol.* V 107: 47-69.
- [21] **Ostwald, J., 1982.** Characterization of Groote Eylandt manganese minerals., *BHP Tech. Bull.* 26: 52 - 56.
- [22] **Burns R.G. and Burns, V.M., 1979.** Manganese oxides. In: R.G. Burns (eds), *Marine Minerals*. Min. Soc. Am., Short Course Notes, 6: 1-40.
- [23] **Ostwald, J., 1988.** Mineralogy of Groote Eylandt manganese oxides: A review. *Ore Geol. Rev.* 4: 3-45
- [24] **Fleischer, M., 1964.** Manganese oxide minerals VIII hollandite. In: *advancing frontier in geology and geophysics (Krishnan Vol.)*, Hyderabad, (Indian Geophysical Union), pp 221-232.
- [25] **Gryaznov, V. I., and Danilov, I. S., 1980.** Oxidized manganese ores of the Nikopol manganese deposit, Ukrainian USSR., In: I. M. Varentsov & G. Grasselly (Eds), *Geology and Geochemistry of Manganese*, 2: 403 - 416.
- [26] **Bar-Matthews, M., 1987.** The genesis of uranium in manganese and phosphorite assemblages, Timna Basin, Israel. *Geol. Mag.* 124: 211-229.
- [27] **Hewett, D.F., 1971.** Coronadite- Modes of occurrence and origin. *Econ. Geol.* 66: 164 - 177.
- [28] **Radcliffe, D., 1974.** Genesis of hypogene psilomelane fibers from the Tower Mine area, New Mexico. *Am. Mineral.* 59: 206 - 207.
- [29] **Frenzel, G., 1980.** The manganese ore minerals. In: Varentsov, I.M. and Grasselly, G. Eds. *Geology and Geochemistry of Manganese* E. Sch. Verl., Stuttgart, 1: 25-158.
- [30] **Sreenivas, B.L. and Roy, R., 1961.** Observations on cation exchange in some manganese minerals by electro dialysis. *Econ. Geol.* 56: 198-203.
- [31] **Mart, J., and Sass, E., 1972.** Geology and origin of the manganese ore of Um Bogma, Sinai. *Econ. Geol.* 67: 145-155.
- [32] **Ostwald, J., 1992.** Mineralogy, paragenesis and

- genesis of the braunite deposits of the Mary Valley Manganese belt, Queensland, Australia. *Mineral. Deposita*, 27: 326-335.
- [33] **Plehwe-Leisen, E.V., and Klemm, D. D., 1995.** Geology and ore genesis of the manganese ore deposits of the Postmasburg manganese-field, South Africa. *Mineral. Deposita*, 30: 257-267.
- [34] **Acharya, B.C., Rao, D.S., and Sahoo, P.R., 1997.** Mineralogy, Chemistry and Genesis of Nishikhal manganese ores of south Orissa, India. *Mineralium Deposita*. 32: 79-93.
- [35] **Ostwald, J. and Bolton, B. R., 1992.** Glauconite Formation as a Factor in Sedimentary Manganese Deposit Genesis. *Econ. Geol.* 87: 1336-1344.
- [36] **Amireh, B.S., 1987.** Sedimentological and Petrological interplays of the Nubian Series in Jordan with regard to paleogeography and diagenesis. Unpublished Ph.D. thesis Diss. 7, University of Braunschweig.
- [37] **Nicholson, K., 1992.** Contrasting Mineralogical-Geochemical Signature of Manganese Oxides: Guides to Metallogenesis. *Econ. Geol.* 87: 1253-1264.
- [38] **Nicholson, K., 1990.** Stratiform manganese mineralisation near Inverness, Scotland: A Devonian sub-lacustrine hot-spring deposit?. *Mineral. Deposita*. 25: 126-131.
- [39] **Kornilovich, I. A., 1968.** Thallium-containing Coronadite from the zone of oxidation of the Ekaterininsk deposit. *Eastern Transbaikal: Vses. Nauchno-Issled. Geol. Inst.Trudy*, 131:33-31.
- [40] **Orcel, J., 1932.** Sur l'existence de la coronadite dans les mineraux de manganese de Bou-Tazoult region de l'Imini (Maroc): *Comptes Rendus Acad. Sci. Paris*. 194: No. 22, 1956-1959.
- [41] **Hewett, D. F., 1964.** Veins of hypogene manganese oxide minerals in the southwestern United States: *Econ. Geol.*, V: 59, No. 8: 1429-1472.

Table 1
Lithology and average thickness of the exposed stratigraphic formations in the study area
along the northern side of Wadi Dana.

Age	Thickness (m)	Formation	Remarks	
Cambrian	Up.	220 - 300	Umm-Ishrin Sandstone	Fine - medium sandstone of continental origin.
	Mid.	45 - 55	DLSU	Manganese main host formation
	Low.	25 - 30	BASU	Traces or remnants of manganese stringers
Upper Precambrian	0 - 50	Hunik Suite, Fidan Suite Ghwayer Volcanics.	Complex basement of quartz-porphyry, syenogranite, and granite.	

Table (2)
Generalized table for all Wadi Dana mineralized sites (from west to east)
showing the ore shapes, degree of crystallinity, and grade.

	Khaled	Dana (Camp)	Jamal	Qusieb	Mahjoob	Dabbah
Ore Shapes	Dissemination, Thin alternating beds. Secondary veins.	Dissemination Irregular Irregular Lenses.	Dissemination Thin alternating beds. Irregular lenses, Veins (LC)	Thin alternating beds, Dissemi- nation	Bands, Lenses, Concertions, Dissemi- nations, Veins (MC)	Thick massive band, Lenses, Dissemination, Veins (MC)
Degree of Crystallinity	Poor	Poor	Poor to Moderate	Poor to Moderate	Good	Good
Average Ore Grade #	4.74	4.65	7.21	3.44	25.6	26.61

LC: Lower Cambrian, MC: Middle Cambrian, #: (Vol. % of Mn).

Table (3)

Selected EPMA data for the high Ba-Todorokite from the study area.

	1	2	3	4
SiO ₂	0.39	0.44	0.29	0.34
Al ₂ O ₃	0.09	0.11	0.14	0.23
TiO ₂	n.d	n.d	n.d	n.d
Fe ₂ O ₃	0.06	0.31	0.1	0.04
MnO ₂	72.44	73.88	70.96	76.01
MgO	0.4	0.56	0.31	0.25
CaO	1.91	3.35	5.03	1.71
Na ₂ O	0.89	0.56	0.22	0.23
K ₂ O	0.09	0.11	0.12	0.17
BaO	15.04	9.84	13.38	14.39
NiO	n.d	n.d	n.d	n.d
CoO	n.d	n.d	n.d	n.d
CuO	0.08	0.07	0.33	0.48
PbO ₂	0.03	0.0	0.02	0.04
ZnO	n.d	n.d	n.d	n.d
Total*	91.42	89.24	90.85	93.89

* H₂O not calculated

Table (4)

Representative EPMA data from the study area for Cryptomelane, Psilomelane, Pyrolusite, and Hollandite.

	1	2	3	4	5	6	7	8	9	10	11	12	13
SiO ₂	0.15	0.1	0.08	0.17	0.45	0.35	0.55	0.09	1.84	1.73	0.99	0.81	0.79
Al ₂ O ₃	0.01	0.21	0.07	0.21	0.23	0.2	0.36	0.06	1.44	1	0.56	0.62	0.75
TiO ₂	0.04	0.05	0.04	n.d	0.33	0.3	0.29	n.d	0.04	0.02	0.06	0.15	0.07
FeO	1.01	0.31	0.15*	0.31*	0.11*	0.11*	0.43	0.11*	0.71*	0.77*	8.34	4.83	3.49
MnO ₂	90.46	90.19	88.9	88.43	79.25	80.05	82.36	84.72	84.73	86.56	73.16	75.91	74.86
MgO	0.013	0.02	0.011	0.004	0.07	0.1	0.03	0.11	0.22	0.11	0.19	0.22	0.18
CaO	0.30	0.16	0.23	0.14	0.2	0.2	0.2	0.59	0.26	0.18	0.53	0.63	0.57
Na ₂ O	0.139	0.28	0.3	0.24	0.21	0.14	0.001	0.23	0.04	0.07	0.16	0.11	0.24
K ₂ O	4.91	5.56	5.16	6.24	0.15	0.13	0.15	1.012	0.27	0.08	0.32	0.71	0.42
BaO	1.11	1.69	1	1.76	15.34	15.13	11.84	2.36	1.07	0/31	3.18	4.56	4.18
NiO	0.02	0.01	n.d	n.dq	n.d	n.d	n.d	n.d	n.d	n.d	0.08	0.06	0.003
CoO	0.01	0.02	n.d	n.d	n.d	n.d	n.d	n.d	n.d	n.d	0.12	0.11	0.14
CuO	1.3	0.82	0.89	0.5	0.89	0.84	0.96	1.9	1.91	1.84	2.14	2.27	2.23
PbO ₂	n.d	n.d.	0.01	0.09	0.04	0.001	0.18	0.13	0.05	0	n.d	n.d	n.d
ZnO	n.d	n.d	0.68	n.d	0.15	0.19	0.49	n.d	0.69	0.8	n.d.	n.d	n.d
Total*	99.47	99.42	97.37	97.78	97.31	97.63	97.84	91.20	92.56	92.39	89.83	90.99	87.92

*Calculated as Fe₂O₃** H₂O was not calculated.

1-4 Cryptomelane, 5-7 Psilomelane, 8-10 Pyrolusite, 11-13 Hollandite.

Table (5)

Selected EPMA data for Coronadite from the study area and other analyses from the world.

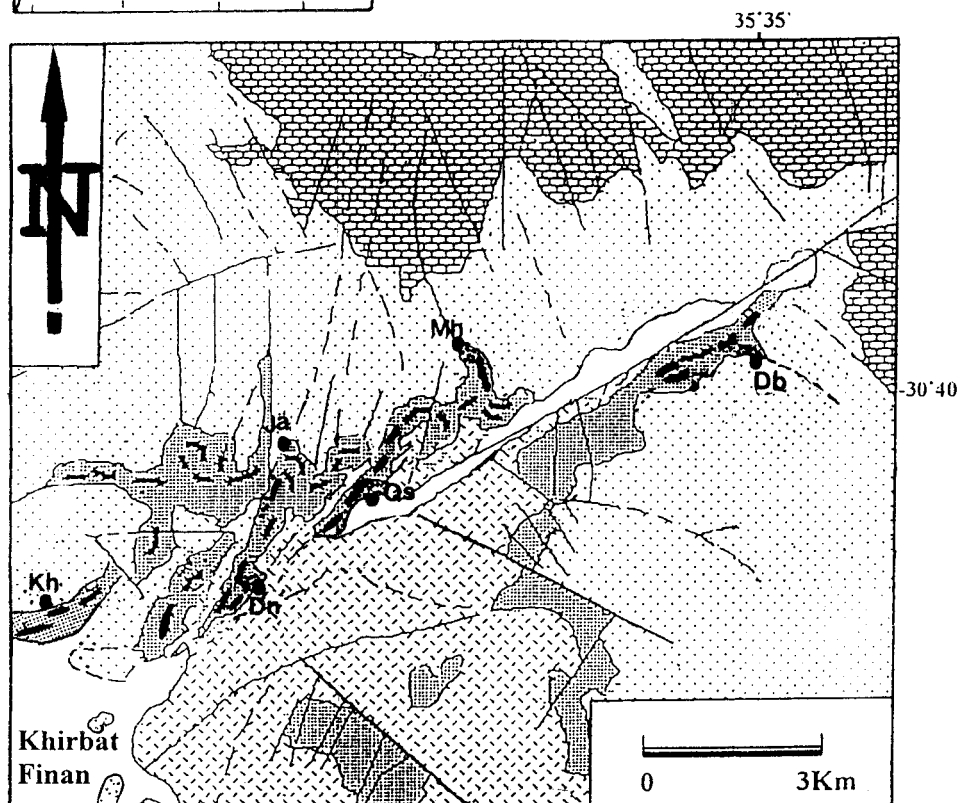
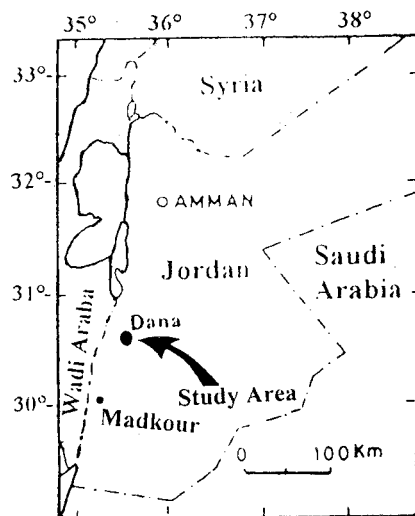
	1	2	3	4	5	6	7	8	9	10
SiO₂	1.9	0.47	0.37	0.49	n.d	n.d	0.75	0.26	0.73	0.38
Al₂O₃	1.27	1.07	0.66	1.19	n.d	n.d	0.04	0.1	1.44	0.39
TiO₂	0.47	0,16	n.d	n.d	n.d	n.d	0.13	0 n.d	0.04	n.d
Fe₂O₃	6.2	0.27	0.65	0.57	9.07	1.7	0.9	0.6	0.33	1.29
MnO₂	55.19	69.66	61.25	75.61	56.97	45.89	54.830	56.8*	58.47*	74.14
MgO	0.13	0.05	0.09	0.01	n.d	n.d	n.d	n.d	0.05	n.d
CaO	0.23	0.14	0.15	0,23	n.d	n.d	n.d	0.05	0.14	n.d
Na₂O	0.12	0.05	0.1	0.34	n.d	n.d	n.d	n.d	0.02	0.14
K₂O	0.3	0.41	0.44	2.88	n.d	n.d	n.d	n.d	0.16	0.42
BaO	3.6	6.47	4.85	4.19	5.69	1.79	3	0.23	3.89	9.98
NiO	n.d	n.d	n.d	n.d	0.008	0.003	n.d	n.d	n.d	n.d
CoO	n.d	n.d	n.d	n.d	0.07	0.02	n.d	n.d	n.d	n.d
CuO	5.15	1.59	n.d	2.4	1.25	0.5	n.d	0.14	0.06	n.d
PbO₂	15.64	11.77	14.79	5.02	3.7	11.55	24.29#	28.68#	20.16#	9.64#
ZnO	0.14	0.1	n.d	n.d	0.21	0.12	1.59	n.d	0.19	0.23
Total \$	90.34	92.05	83.35	92.7	76.968	61.573	85.53	86.86	85.68	96.61

1-4: Study area, **5&6:** Coronadite, Timna Israel (Bar Matthews, 1987) [26] (Samples 6405+6432 was recalculated as oxides by the authors), **7:** Coronadite Ekaterininsk, Transbaikalia, USSR, (Kornilovich, 1968) [39], **8:** Coronadite, Bou Tazoult, Morocco (Orcel, 1932) [40], **9:** Coronadite, Luis Lopez, New Mexico (Hewett, 1964) [41]), **10:** Pb-hollandite, Yucca Mts, Nevada, USA (Carlos et al., 1993) [20].

*Calculated as MnO

Calculated as PbO

\$ H₂O was not calculated



LEGEND:


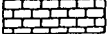
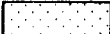

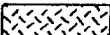
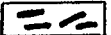

- | | | | |
|---|----------------------|---|----------------------------------|
|  | Wadi Sediments |  | Cretaceous – Tertiary |
|  | Paleozoic Sediments |  | Lower-Middle Cambrian Formations |
|  | Precambrian Basement |  | Manganese Mineralization |
|  | Sampling Sites | | |

Fig. (1)

Location and Geological Map of the Study Area, Modified after (Humrat Fidan & Ash-Shoubak sheets), NRA - Amman.

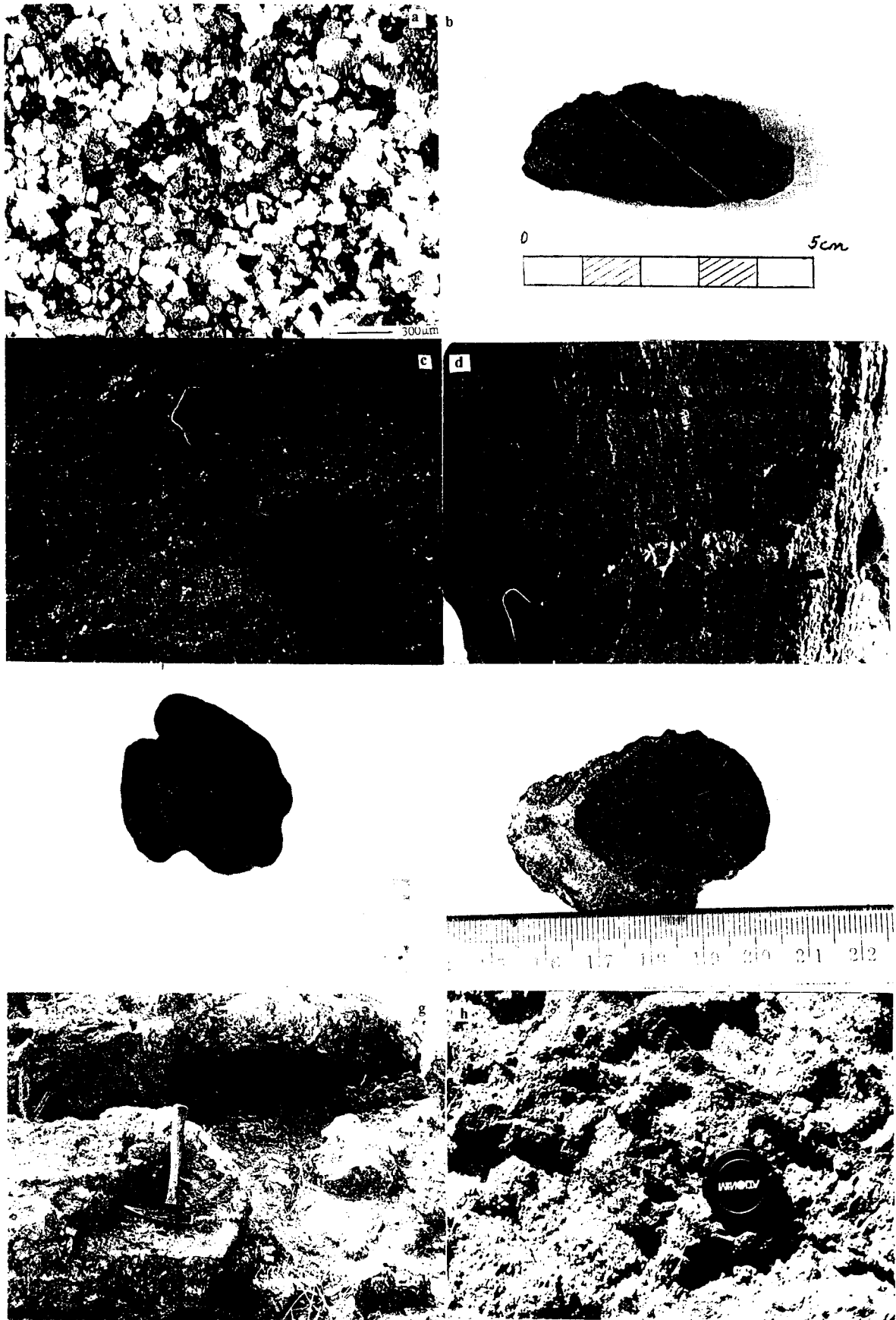


Fig. (2)

(a) Reflected light figure showing the manganese minerals cementing sandstone grains. (b) Honeybee texture of disseminated ore type in dolomitic sandstone. (c) Lenses and broken lenses embedded in clay layers. (d) Thin manganese layers alternating the siltstone and claystone layers. (e) Multi-nodules of manganese oxides. (f) Layering in manganese nodules showing the core (nucleus). (g) Massive band ore at Wadi Dabbah. (h) Stock-work veins of manganese oxide in the sandstone.

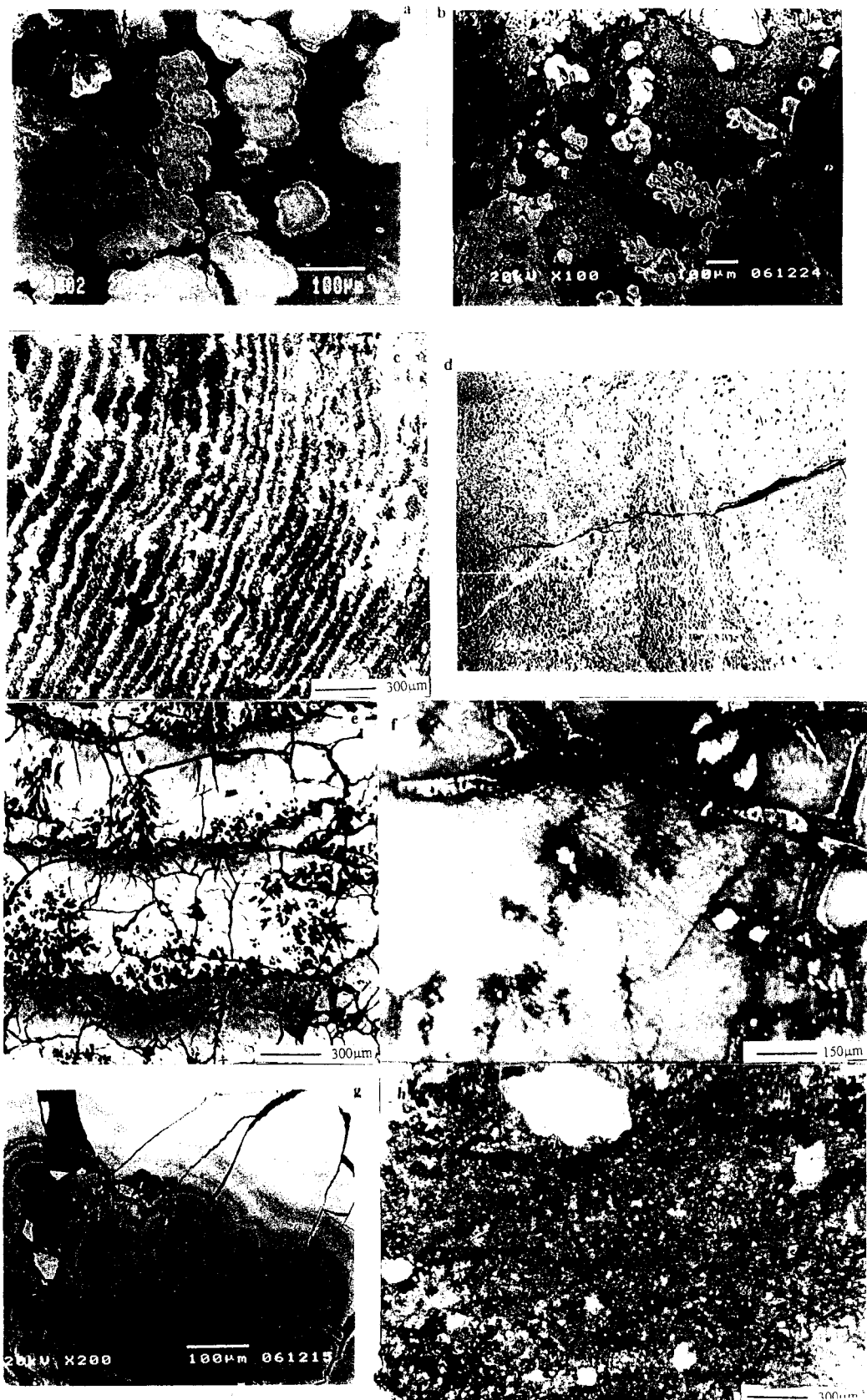


Fig. (3)

SEM figure showing the Mn ooids embedded in the calcareous matrix. (b) Primary oolitic texture is overprinted by the newly formed supergene minerals (psilomelane, white spots). (c) Reflected light figure showing the Ring-Wood texture between pyrolusite and psilomelane, cross section of nodule. (d) SEM figure showing the secondary psilomelane veins invading the matrix of cryptomelane and early-diagenetic psilomelane. (e) Reflected light figure showing the Fish-scale texture between pyrolusite (with black dendritic inclusions) and hematite. (f) Transmitted light figure showing the epigenetic coronadite associating chrysocolla. (g) SEM figure showing the well-crystallized coronadite of Wadi Mahjoob. (h) Transmitted light figure showing secondary manganese veinlets (denticles) invading dolomite.

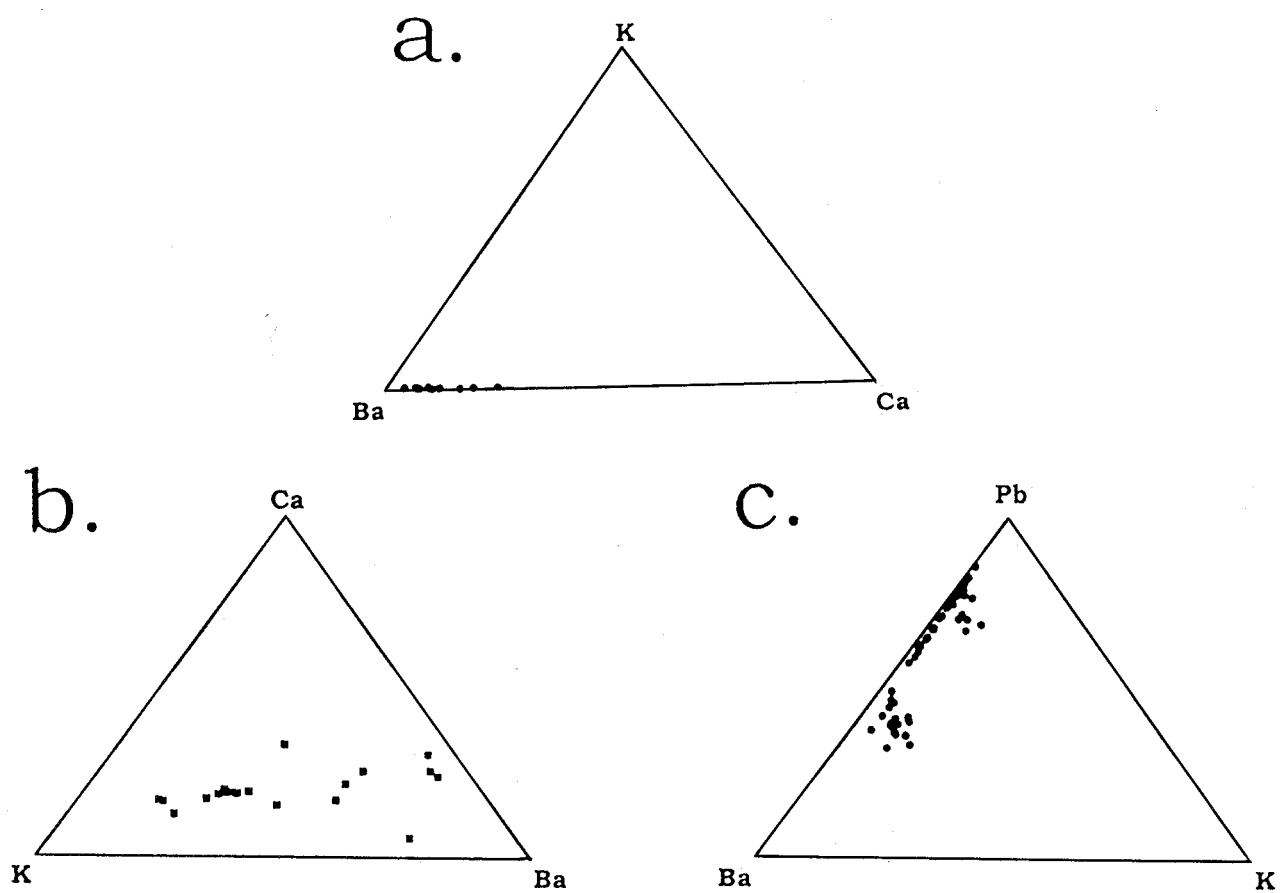


Fig. (4)

Ternary plotting based on EPMA data for the ore minerals showing series of solid solutions (a) Todorokite - Psilomelane. (b) Cryptomelane - Psilomelane. (c) Hollandite - Coronadite.

	Primary Sedimentary	Secondary Supergene		Epigenetic Lateritization
		Early Diagenetic	Late Diagenetic	
Quartz	-----			
Dolomite	-----			
Kaolinite	-----			
Todorokite	-----			
Birnessite	-----			
Manganite	-----			
Apatite	-----			
Cryptomelane		-----	-----	
Psilomelane		-----	-----	-----
Hollandite		-----	-----	
Pyrolusite		-----	-----	
Hematite		-----	-----	-----
Goethite			-----	-----
Barite			-----	-----
Calcite		-----	-----	-----
Kutonaohorite		-----		
Ankerite		-----		
Coronadite				-----

Fig. (5)

Paragenetic sequence of Wadi Dana manganese ore deposits, including the gangue minerals.